

Flow in pPb collisions at 5 TeV?

K. Werner^(a), B. Guiot^(a), Iu. Karpenko^(b,c), T. Pierog^(d)

^(a) *SUBATECH, University of Nantes – IN2P3/CNRS– EMN, Nantes, France*

^(b) *Bogolyubov Institute for Theoretical Physics, Kiev 143, 03680, Ukraine*

^(c) *FIAS, Johann Wolfgang Goethe Universitaet, Frankfurt am Main, Germany*

^(d) *Karlsruhe Inst. of Technology, KIT, Campus North, Inst. f. Kernphysik, Germany*

There is little doubt that hydrodynamic flow has been observed in heavy ion collisions at the LHC and RHIC, mainly based on results on azimuthal anisotropies, but also on particle spectra of identified particles, perfectly compatible with hydrodynamic expansions. Surprisingly, in p-Pb collisions one observes a very similar behavior. So do we see flow even in p-Pb? We will try to answer this question.

Collective hydrodynamic flow seems to be well established in heavy ion (HI) collisions at energies between 200 and 2760 AGeV, whereas p-p and p-nucleus (p-A) collisions are often considered to be simple reference systems, showing “normal” behavior, such that deviations of HI results with respect to p-p or p-A reveal “new physics”. Surprisingly, the first results from p-Pb at 5 TeV on the transverse momentum dependence of azimuthal anisotropies and particle yields are very similar to the observations in HI scattering^{1,2}.

Do we see radial flow in p-Pb collisions? In order to answer this question, we will employ the EPOS3 approach³, well suited for this problem, since it provides within a unique theoretical scheme the initial conditions for a hydrodynamical evolution in p-p, p-A, and HI collisions. The initial conditions are generated in the Gribov-Regge multiple scattering framework. An individual scattering is referred to as Pomeron, identified with a parton ladder, eventually showing up as flux tubes (also called strings). Each parton ladder is composed of a pQCD hard process, plus initial and final state linear parton emission. Our formalism is referred to as “Parton based Gribov Regge Theory” and described in very detail in⁴. Based on these initial conditions, we performed already ideal hydrodynamical calculations (EPOS2)^{5,6,7,8} to analyse HI and p-p scattering at RHIC and LHC. In EPOS3 we add two major improvements: a more sophisticated treatment of nonlinear effects in the parton evolution by considering individual (per Pomeron) saturation scales⁹, and a 3D+1 viscous hydrodynamical evolution. There are also changes in our core-corona procedure, which amounts to separate the initial energy of the flux tubes into a part which constitutes the initial conditions for hydro (core) and the particles which leave the “matter”. This is crucial as well in proton-nucleus collisions (as in all other collision types).

To understand the results discussed later in this paper, we show in fig. 1 the effect of flow on identified particle spectra, by comparing p_t distributions from pure string decay to spectra from a pure hydrodynamic evolution. In case of string fragmentation, heavier particles are strongly suppressed compared to lighter ones, but the shapes are not so different. This picture changes

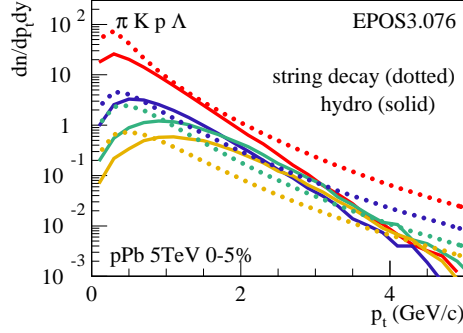


Figure 1 – (Color online) Identified particle spectra as a function of p_t , for central (0-5%) p-Pb collisions at 5.02 TeV. We show results for particle production from string decay, i.e. EPOS without hydro (dotted curves), and particle production from pure hydro, without corona (solid lines). In both cases, we show (from top to bottom) pions, kaons, protons, and lambdas.

completely in the fluid case: The heavier the particle, the more it gets shifted to higher p_t . This is a direct consequence of the fact that the particles are produced from fluid cells characterized by radial flow velocities, which gives more transverse momentum to heavier particles.

There are few other studies of hydrodynamic expansion in proton-nucleus systems. In ¹⁰, fluctuating initial conditions based on the so-called Monte Carlo Glauber model (which is actually a wounded nucleon model) are employed, followed by a viscous hydrodynamical evolution. Also ¹¹ uses fluctuating initial conditions, here based on both Glauber Monte Carlo and Glasma initial conditions. Finally in ¹², ideal hydrodynamical calculations are performed, starting from smooth Glauber model initial conditions.

In the following, we will compare experimental data on identified particle production with our simulation results (referred to as EPOS3), and in addition to some other models, as there are QGSJETII ¹³, AMPT ¹⁴, and EPOS LHC ¹⁵. The QGSJETII model is also based on Gribov-Regge multiple scattering, but there is no fluid component. The main ingredients of the AMPT model are a partonic cascade and then a hadronic cascade, providing in this way some “collectivity”. EPOS LHC is a tune (using LHC data) of EPOS1.99. As all EPOS1 models, it contains flow, put in by hand, parametrizing the collective flow at freeze-out. Finally, the approach discussed in this paper (EPOS3) contains a full viscous hydrodynamical simulation. So it is interesting to compare these four models, since they differ considerably concerning the implementation of flow, from full hydrodynamical flow in EPOS3 to no flow in QGSJETII.

The CMS collaboration published a detailed study ¹ of the multiplicity dependence of (normalized) transverse momentum spectra in p-Pb scattering at 5.02 TeV. The multiplicity (referred to as N_{track}) counts the number of charged particles in the range $|\eta| < 2.4$. In fig. 2, we compare experimental data ¹ for pions (black symbols) with the simulations from QGSJETII (upper left figure), AMPT (upper right), EPOS LHC (lower left), and EPOS3 (lower right). The different curves in each figure refer to different centralities, with mean values (from bottom to top) of 8, 84, 160, and 235 charged tracks. They are shifted relative to each other by a constant amount. Concerning the models, QGSJETII is the easiest to discuss, since here there are no flow features at all, and the curves for the different multiplicities are identical. The data, however, show a slight centrality dependence: the spectra get somewhat harder with increasing multiplicity. The other models, AMPT, EPOS LHC, and EPOS3 are close to the data.

In figs. 3, 4, we compare experimental data ¹ for kaons and protons (black symbols) with the simulations. The experimental shapes of the p_t spectra change considerably, getting much harder with increasing multiplicity. In QGSJETII, having no flow, the curves for the different multiplicities are identical. The AMPT model shows some (but too little) change with multiplicity. EPOS LHC goes into the right direction, whereas EPOS3 gives a reasonable description of the data. **It seems that hydrodynamical flow helps considerably to reproduce these**

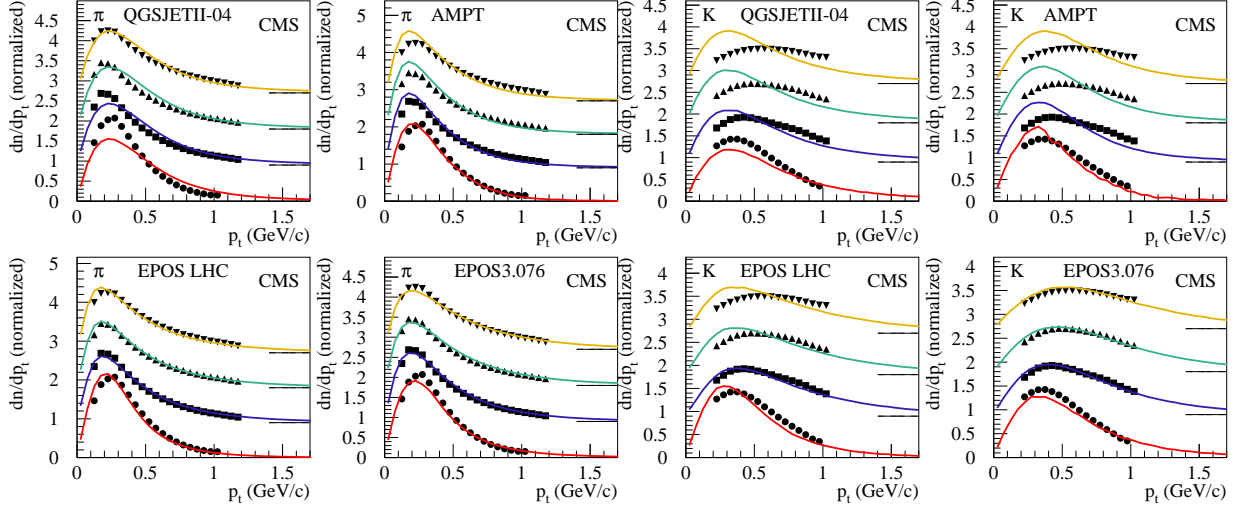


Figure 2 – (Color online) Transverse momentum spectra of pions in p-Pb scattering at 5.02 TeV, for four different multiplicity classes with mean values (from bottom to top) of 8, 84, 160, and 235 charged tracks.

Figure 3 – (Color online) Same as fig. 2, but for kaons. We show data from CMS (symbols) and simulations from QGSJETII, AMPT, EPOS LHC, and EPOS3, as indicated in the figures.

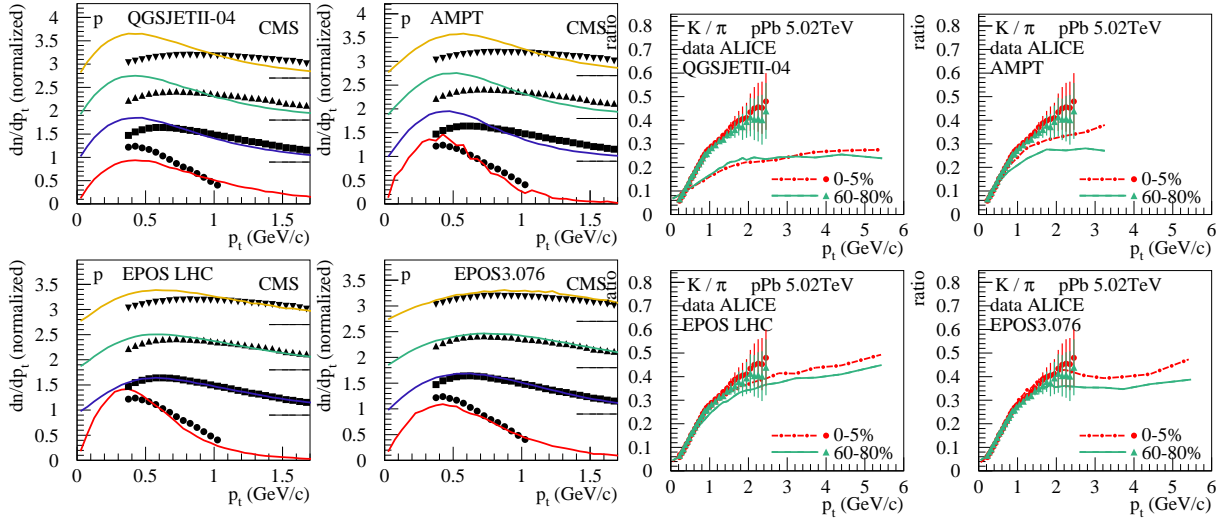


Figure 4 – (Color online) Same as fig. 2, but for protons.

Figure 5 – (Color online) Kaon over pion ratio as a function of transverse momentum in p-Pb scattering at 5.02 TeV, for the 0-5% highest multiplicity (red dashed-dotted lines, circles) and 60-80% (green solid lines, triangles).

data.

Also ALICE² has measured identified particle production for different multiplicities in p-Pb scattering at 5.02 TeV. Here, multiplicity counts the number of charged particles in the range $2.8 < \eta_{\text{lab}} < 5.1$. It is useful to study the multiplicity dependence, best done by looking at ratios. In fig. 5, we show the pion over kaon (K/π) ratio as a function of transverse momentum in p-Pb scattering at 5.02 TeV, for high multiplicity (red dashed-dotted lines, circles) and low multiplicity events (green solid lines, triangles), comparing data from ALICE² (symbols) and simulations from QGSJETII, AMPT, EPOS LHC, and EPOS3 (lines). In all models, as in the data, there is little multiplicity dependence. However, the QGSJETII model is considerably below the data, for both high and low multiplicity events. AMPT is slightly below, whereas EPOS LHC and EPOS3 do a reasonable job. Concerning the proton over pion (p/π) ratio, fig. 6,

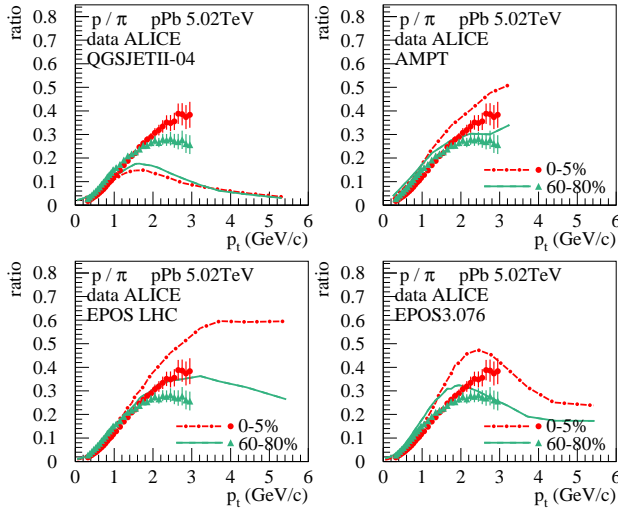


Figure 6 – (Color online) Same as fig. 5, but proton over pion ratio.

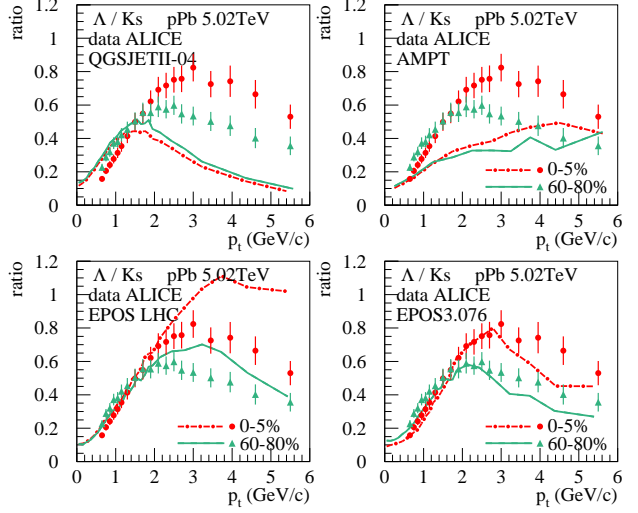


Figure 7 – (Color online) Same as fig. 5, but Λ over K_s ratio.

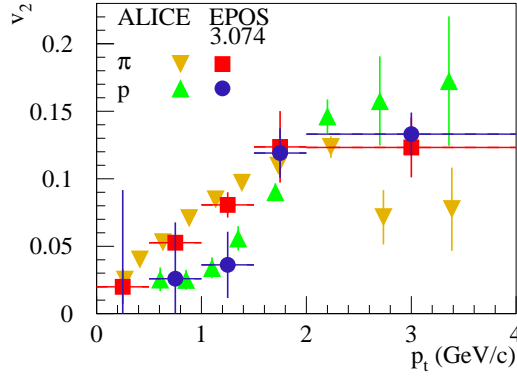


Figure 8 – (Color online) Elliptical flow coefficients v_2 for pions and protons. We show ALICE results (triangles) and EPOS3 simulations (squares and circles). Pions appear red and yellow, protons blue and green.

again QGSJETII is way below the data, for both high and low multiplicity events, whereas the three other models show the trend correctly, but being slightly above the data. Most interesting are the lambdas over kaon (Λ/K_s) ratios, as shown in fig. 7, because here a wider transverse momentum range is considered, showing a clear peak structure with a maximum around 2-3 GeV/c and a slightly more pronounced peak for the higher multiplicities. QGSJETII and AMPT cannot (even qualitatively) reproduce this structure. EPOS LHC shows the right trend, but the peak is much too high for the high multiplicities. EPOS3 is close to the data.

To summarize these ratio plots (keeping in mind that the QGSJETII model has no flow, AMPT “some” flow, EPOS LHC a parametrized flow, and EPOS3 hydrodynamic flow): Flow seems to help considerably. However, from the Λ/K_s ratios, we conclude that EPOS LHC uses a too strong radial flow for high multiplicity events. The hydrodynamic flow employed in EPOS3 seems to get the experimental features reasonably well. Crucial is the core-corona procedure discussed earlier: there is more core (compared to corona) in more central collisions, but the centrality (or multiplicity) dependence is not so strong, and there is already an important core (=flow) contribution in peripheral events.

Finally, we sketch very briefly results on elliptical flow v_2 obtained from dihadron correlations, showing ALICE results^{16,17} and EPOS3 simulation, see ref.¹⁸ for details. In fig. 8. we plot v_2 as a function of p_t . Clearly visible in data and in the simulations: a separation of the results for the two hadron species: in the p_t range of 1-1.5 GeV/c, the proton result is clearly

below the pion one. Within our fluid dynamical approach, the above results are nothing but a “mass splitting”. The effect is based on an asymmetric (mainly elliptical) flow, which translates into the corresponding azimuthal asymmetry for particle spectra. Since a given velocity translates into momentum as $m_A \gamma v$, with m_A being the mass of hadron type A , flow effects show up at higher values of p_t for higher mass particles.

To summarize : Comparing experimental data on identified particle production to various Monte Carlo generators, we conclude that hydrodynamical flow seems to play an important role in p-Pb scattering.

This research was carried out within the scope of the GDRE (European Research Group) “Heavy ions at ultrarelativistic energies”. Iu.K acknowledges support by the National Academy of Sciences of Ukraine (Agreement 2014) and by the State Fund for Fundamental Researches of Ukraine (Agreement 2014). Iu.K. acknowledges the financial support by the ExtreMe Matter Institute EMMI and the LOEWE initiative of the State of Hesse. B.G. acknowledges the financial support by the TOGETHER project of the Region of “Pays de la Loire”.

1. CMS collaboration, arXiv:1307.3442
2. ALICE collaboration, arXiv:1307.6796
3. K. Werner et al., to be published
4. H. J. Drescher, M. Hladik, S. Ostapchenko, T. Pierog and K. Werner, Phys. Rept. 350, 93, 2001
5. K. Werner, Iu. Karpenko, T. Pierog, M. Bleicher, K. Mikhailov, Phys. Rev. C 82, 044904 (2010)
6. K. Werner, Iu. Karpenko, M. Bleicher, T. Pierog, S. Porteboeuf-Houssais, arXiv:1203.5704, Phys. Rev. C 85 (2012) 064907
7. K. Werner, Iu. Karpenko, T. Pierog, M. Bleicher, K. Mikhailov, arXiv:1010.0400, Phys. Rev. C 83, 044915 (2011)
8. K. Werner, Iu. Karpenko, T. Pierog, arXiv:1011.0375, Phys. Rev. Lett. 106, 122004, 2011
9. L. McLerran, R. Venugopalan, Phys. Rev. D 49 (1994) 2233; L. McLerran, R. Venugopalan, Phys. Rev. D 49 (1994) 3352; L. McLerran, R. Venugopalan, Phys. Rev. D 50 (1994) 2225.
10. P. Bozek, W. Broniowski, arXiv:1304.3044
11. A. Bzdak, B. Schenke, P. Tribedy, R. Venugopalan, arXiv:1304.3403
12. G.Y. Qin, B. Mueller, arXiv:1306.3439
13. S. Ostapchenko, Phys. Rev. D 74 (2006) 014026; S. Ostapchenko, Phys. Rev. D 83 (2011) 014018
14. Z.-W. Lin, C. M. Ko, B.-A. Li, B. Zhang and S. Pal, Phys. Rev. C 72, 064901 (2005).
15. T. Pierog, Iu. Karpenko, J.M. Katzy, E. Yatsenko, K. Werner, arXiv:1306.5413.
16. ALICE collaboration, Phys. Lett. B 719 (2013) 29-41, arXiv:1212.2001
17. ALICE collaboration, preprint CERN-PH-EP-2013-115 arXiv:1307.4379
18. K. Werner, M. Bleicher, B. Guiot, Iu. Karpenko, T. Pierog, arXiv:1307.4379 [nucl-th]